

## Supramolecular inclusion complexes of 2-hydroxypropyl- $\beta$ -cyclodextrin with mefenamic acid: preparation and characterization

*G.V.Grygorova<sup>1</sup>, V.K.Klochkov<sup>1</sup>, N.A.Kasian<sup>1</sup>,  
P.V.Mateychenko<sup>2</sup>, D.S.Sofronov<sup>3</sup>, S.L.Yefimova<sup>1</sup>*

<sup>1</sup>Institute for Scintillation Materials, STC "Institute for Single Crystals", National Academy of Sciences of Ukraine, 60 Nauky Ave., 61072 Kharkiv, Ukraine

<sup>2</sup>Institute for Single Crystals, STC "Institute for Single Crystals", National Academy of Sciences of Ukraine, 60 Nauky Ave., 61072 Kharkiv, Ukraine

<sup>3</sup>SSI "Institute for Single Crystals", National Academy of Sciences of Ukraine, 60 Nauky Ave., 61072 Kharkiv, Ukraine

*Received July 29, 2021*

We report the synthesis and evaluation of inclusion complexes between mefenamic acid (MFA) and 2-hydroxypropyl- $\beta$ -cyclodextrin (HP- $\beta$ -CD). The phase solubility studies reveal that MFA forms a complex with the HP- $\beta$ -CD at a 1:1 molar ratio that was also confirmed by UV-vis spectral data (Job's plots). Characterizations of the prepared host-guest type solid complexes using a reliable spectroscopic and calorimetric methods indicate that MFA is found inside the cavity of the HP- $\beta$ -CD. Obtained thermodynamic parameters for MFA/HP- $\beta$ -CD complex formation show that MFA inclusion in HP- $\beta$ -CD cavities is favorable, spontaneous exothermic and enthalpy-driven process. The stability constant  $K_s$  for MFA/HP- $\beta$ -CD complexes determined from the Benesi-Hildebrand equation using fluorescence spectral data is adequate for the formation of an inclusion complex indicates that a fast MFA drug release from MFA/HP- $\beta$ -CD complex should be expected. The presented results show the MFA/HP- $\beta$ -CD complex as an effective new approach to design a novel formulation for pharmaceutical applications.

**Keywords:** 2-hydroxypropyl- $\beta$ -cyclodextrin, mefenamic acid, inclusion complexes, phase solubility, stability constant.

**Супрамолекулярні комплекси включення 2-гідроксипропил- $\beta$ -циклодекстрину з мефенаміновою кислотою: отримання та характеристика.** Г.В.Григорова, В.К.Клочков, Н.О.Касян, П.В.Матейченко, Д.С.Софронів, С.Л.Ефімова

Проведено синтез та оцінку комплексів включення між мефенаміновою кислотою (МФК) та 2-гідроксипропил- $\beta$ -циклодекстрином (ГП- $\beta$ -ЦД). Дослідженням фазової розчинності виявлено, що МФК утворює комплекс із ГП- $\beta$ -ЦД у молярному співвідношенні 1:1, і підтверджено даними УФ-спектроскопії (графіки Джоба). Характеристики отриманих твердих комплексів типу "господар-гість" з використанням надійних спектроскопічних та калориметричних методів виявляють, що МФК знаходиться всередині порожнини ГП- $\beta$ -ЦД. Отримані термодинамічні параметри вказують на те, що включення молекул кислоти у порожнину циклодекстрину є сприятливим, самовільним екзотермічним та ентальпійним процесом. Константу стабільності для комплексів МФК/ГП- $\beta$ -ЦД визначено за рівнянням Бенеші-Хільдебранда з використанням спектральних даних за флуоресценцією, вона є адекватною для утворення комплексу включення, що вказує на те, що можна очікувати швидке вивільнення лікарського засобу МФК із комплексу МФК/ГП  $\beta$ -ЦД.

Проведены синтезе и оценка комплексов включения между мефенаминовой кислотой (МФК) и 2-гидроксипропил- $\beta$ -циклодекстрином (ГП- $\beta$ -ЦД). Исследования фазовой растворимости показывают, что МФК образует комплекс с ГП- $\beta$ -ЦД в молярном соотношении 1:1, что также подтверждено данными УФ спектроскопии (графики Джоба). Характеристики полученных твердых комплексов типа "хозяин-гость" с использованием надежных спектроскопических и калориметрических методов показывают, что МФК находится внутри полости ГП- $\beta$ -ЦД. Полученные термодинамические параметры показывают, что включение молекулы кислоты в полость циклодекстрина является благоприятным, самопроизвольным экзотермическим и энтальпийным процессом. Константа стабильности для комплексов МФК/ГП- $\beta$ -ЦД, определенная по уравнению Бенеша-Хильдебранда с использованием спектральных данных по флуоресценции, является адекватной для образования комплекса включения, что указывает на то, что можно ожидать быстрое высвобождение лекарственного средства МФК из комплекса МФК /ГП- $\beta$ -ЦД.

### 1.Introduction

Non-steroidal anti-inflammatory drugs (NSAIDs) constitute an important class of compounds to alleviate inflammation and pain associated with disease or injury etc.; they exert their therapeutic effects by inhibiting the release of prostaglandin and thromboxane hormone produced in human body by enzymatic transformation [1–3]. Mefenamic acid (2-[N-(2,3-dimethylphenyl)amino]benzoic acid, MFA), which structural formula is shown in Fig. 1a, belongs to a family of NSAIDs with antipyretic and strong analgesic properties which is a derivative of N-phenylanthranilic acid. This compound is of specific interest because of its biological activity-it is a potential inhibitor of prostaglandin synthesis, the presence of which is closely associated with inflammatory processes [4]. Also, mefenamic acid has shown neuroprotective effects, therapeutic effects in neurodegeneration Alzheimer's disease and anticancer agents (particularly colon and liver cancer cell lines) [5–8]. However, the poor water solubility of MFA causes difficulties related to the design of pharmaceutical formulations for oral or parenteral route administration, leading thus to low oral bioavailability. The aqueous solubility of mefenamic acid at pH 7.1 is 0.0041 g/100 ml (25°C) and 0.008 g/100 ml (37°C) [9].

Drug dissolution in gastric and intestinal fluids is an essential step for drug absorption in the human body and ultimately a therapeutic effect [10, 11]. So, poor dissolution leads to limited absorption resulting in lower plasma concentrations than expected. Higher doses of drugs are often given to achieve the desired plasma concentration which eventually will result in adverse effects. These side-effects have a negative impact on patient compliance [12]. This area poses the challenge for the pharmaceutical

industry to discover new methods to increase solubility and, therefore, potentially bioavailability. Complexation with cyclodextrins is an approach that can be used to solve this problem.

Recently cyclodextrins (CDs), being regularly built cyclic oligosaccharides, have been intensively used as an auxiliary substance in biochemical researches and pharmacology, mainly, for the encapsulation of different drugs. Such encapsulation usually protects drugs from biodecomposition, promotes its solubility in water promoting the effective and selective target drug delivery [13–15]. It is necessary to mark that  $\beta$ -cyclodextrin ( $\beta$ -CD) appears to be the best natural cyclodextrin for pharmaceutical applications due to its efficient drug complexation, but relatively low aqueous solubility (1.85 g/100 mL) [16] and nephrotoxicity limited his use in pharmaceutical compositions [17, 18]. To overcome indicated problems CDs are subjected to various chemical modifications. Some chemically modified CDs such as 2-hydroxypropyl- $\beta$ -cyclodextrin (HP- $\beta$ -CD) includes seven D-glycopyranose fragments, containing hydroxypropyl groups in the positions 2, 3, and 6. HP- $\beta$ -CD is a more water-soluble and less toxic than naturally occurring  $\beta$ -CD (Fig. 1b) [19]. The HP- $\beta$ -CD has a hydrophobic central cavity and a hydrophilic outer surface and can encapsulate various inorganic/organic molecules of appropriated sizes and polarity to form host-guest complexes or supramolecular species. According to literature, the main forces involved in the inclusion of guest molecules into the CD cavity are van der Waals, hydrogen bonding, hydrophobic interactions, electrostatic interactions, charge-transfer interactions, release of bond water from CD cavity [20–22].

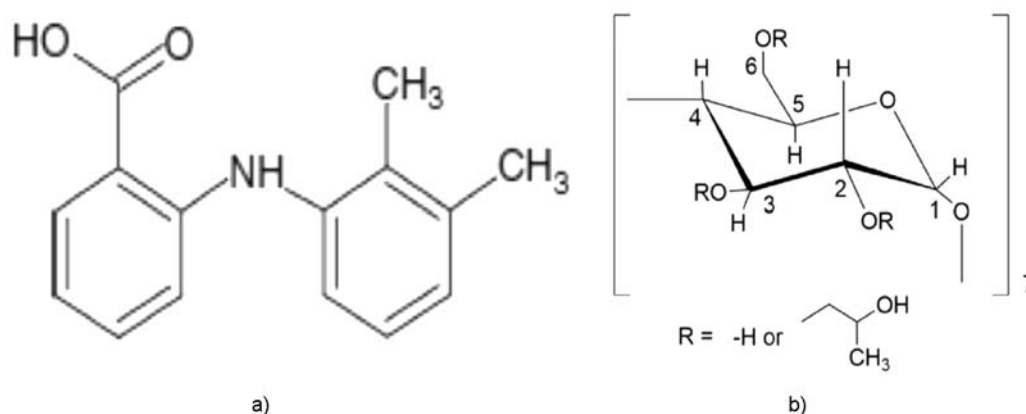


Fig. 1. Chemical structure of mefenamic acid (a) and 2-hydroxypropyl-β-cyclodextrin (b).

Recently various studies involving inclusion complexation phenomena have been reported for new generation of NSAIDs, which are almost insoluble in water, primarily to enhance the oral bioavailability and dissolution behavior [23, 24].

The objective of this study was to carry out a systematic investigation of the host-guest complexation between MFA and HP-β-CD in both liquid and solid states. The evaluation of MFA/HP-β-CD complex formation and its stoichiometry and stability in both states have been examined by variety of methods and indicates that this method is prospective to increase MFA stability and bioavailability.

## 2. Experimental

### 2.1 Materials

2-Hydroxypropyl-β-cyclodextrin (MW ~ 1396) and mefenamic acid (MW~241.28) were purchased from Sigma-Aldrich (Saint Louis, MO, USA) and used as supplied. Universal buffer (pH = 7.5) was prepared using acetic acid, boric acid, phosphoric acid (0.04 M) solution titrated with 0.2 M NaOH. All other chemicals were of reagent grade, and deionized water was used throughout the experiments.

### 2.2 Preparation of inclusion complexes of MFA with HP-β-CD in solution

The stock  $4 \cdot 10^{-4}$  M solution of mefenamic acid was prepared by dissolving the powder in 10 ml of 0.2 M NaOH followed by adjusting the acidity of the MFA solution to pH 7.5 using a universal buffer mixture of acids. Exactly 1 ml of this stock solution was transferred into each of the 10 ml volumetric flasks, and different concentrations of HP-β-CD solution (ranging from  $1.0 \cdot 10^{-3}$  to  $2 \cdot 10^{-2}$  M) were added. The mixed solution was diluted to 10 ml with deionized water and shaken

thoroughly. The final concentration of the drug in all the flasks was  $4 \cdot 10^{-5}$  M. The solutions were prepared just before each measurement.

### 2.3 Preparation of lyophilized inclusion complexes of MFA with HP-β-CD

The lyophilized inclusion complex of MFA with HP-β-CD (MFA/HP-β-CD) was prepared by the co-evaporation method. Co-evaporated systems at molar ratios of 1:1 (MFA to HP-β-CD) were obtained by dissolving calculated amount of MFA in 5 mL of ethanol and HP-β-CD in 20 mL of ethanol. MFA solution was slowly added to the HP-β-CD solution with continuous agitation for 4 h at 25°C. Then the mixed solution was titrated with 0.1 M NaOH to obtain the solution with the pH is 10. Ethanol was then removed using a rotary vacuum evaporator at 55°C. The obtained white powders were dried and stored in a desiccator for 24 h, after the samples were transferred in sealed glass containers for further investigation.

**Physical mixtures:** A physical mixture of MFA and HP-β-CD (at the same molar ratios) were prepared by thoroughly mixing the two components in an agate mortar for 30 min.

### 2.4 Phase solubility studies

Phase solubility studies of MFA and HP-β-CD were carried out by the method of Higuchi and Conors at room conditions [25]. Excess amount of MFA was added to screw capped vials containing various concentrations of HP-β-CD solutions (from 0 to 0.1 M). These solutions were stirred during 48 h at room conditions. After equilibrium was attained, the solutions were filtered through 0.45 μm membrane fillters to remove undissolved solid. An aliquot from each vial was diluted by alcohol and the

concentration of MFA was analyzed using SPECORD 200 spectrophotometer at characteristic wavelength  $\lambda_{max} = 286$  nm. The calibration curve of MFA absorption in water solutions was established.

The apparent stability constants ( $K_s$ ) of the complexes were calculated from the phase-solubility diagrams according to the following Eq. (1):

$$K_s = \frac{Slope}{S_0(1 - Slope)}, \quad (1)$$

where  $K_s$  is the apparent stability constant of the MFA/HP- $\beta$ -CD inclusion complex and  $S_0$  is the apparent solubility of free MFA without HP- $\beta$ -CD in aqueous solution, which can be obtained from the straight-line of the phase solubility diagram.

Complexation efficiency ( $CE$ ) was defined as the solubilizing efficiency of CDs for guest molecule. Based on the results of the phase solubility studies,  $CE$  of HP- $\beta$ -CD for MFA was determined using the following Eq. (2):

$$CE = \frac{\left[\frac{MFA}{HP} - \beta - CD\right]}{[HP - \beta - CD]} = , \quad (2)$$

$$= S_0 \times K_s = \frac{Slope}{S_0(1 - Slope)}$$

where [MFA/HP- $\beta$ -CD] referred to the concentration of the inclusion complex and [HP- $\beta$ -CD] was the concentration of free HP- $\beta$ -CD and  $Slope$  is the slope of the phase solubility profile [26].

#### 2.5 Spectroscopic measurements

MFA/HP- $\beta$ -CD complex formation was monitored by UV-Vis spectroscopy. The absorption spectra were measured with a SPECORD 200 (Analytik Jena) spectrophotometer. Measurements were done at room temperature ( $25 \pm 0.5^\circ\text{C}$ ) in the spectral range of 220–450 nm. The fluorescence spectra were measured with a Lumina (Thermo Scientific) spectrofluorimeter. The excitation and emission wavelengths were 350 and 400 nm, respectively. For registration of the absorption spectra and fluorescence spectra, a quartz cuvette with an optical path length of 1.0 cm was used.

#### 2.6 Scanning Electron Microscopy (SEM)

The morphology of HP- $\beta$ -CD, MFA and the inclusion complex were recorded using a scanning electron microscopy SEM JSM-6390LV (JEOL Company, USA). The powder samples were fixed on a silicone supports.

The samples were scanned by an electron beam of acceleration potential of 15 kV.

#### 2.7 Fourier-transform infrared spectroscopy (FTIR)

Infrared (IR) spectra of the samples (MFA, HP- $\beta$ -CD, inclusion complexes and physical mixtures) were recorded in the range of 400–4000  $\text{cm}^{-1}$  using Spectrum One (PerkinElmer) IR-Fourier spectrophotometer. The samples were previously mixed thoroughly with KBr.

#### 2.8 Differential scanning calorimetry (DSC)

The differential scanning calorimetry studies were performed using a DSC 1 calorimeter (Mettler Toledo, Switzerland). The samples (approx. 7 mg) were placed in flat-bottomed aluminum crucibles and heated at a scan rate of  $10^\circ\text{C min}^{-1}$  in the range of 25–300 $^\circ\text{C}$  under a nitrogen purge. The DSC thermograms were processed using a DSC 1 calorimeter software.

#### 2.9 Thermal gravimetric analysis (TGA)

The content of volatile impurities was determined by the methods of thermogravimetric analysis using a Mettler TA 3000 thermoanalytical device (Mettler, Switzerland). A 20 mg sample was incubated at a temperature of 105 $^\circ\text{C}$  for two hours in an open aluminum oxide crucible with a volume of 160  $\mu\text{L}$ . Each obtained thermogram contained about 600 experimental points. The specific weight loss (as a percentage of the initial mass of the substance) was determined immediately after the drying of the sample (at 105 $^\circ\text{C}$ ), after cooling down the sample to room temperature (at 30 $^\circ\text{C}$ ), and also 24 h after the end of the experiment.

#### 2.10 Determination of MFA/HP- $\beta$ -CD complex stoichiometry

The stoichiometry of the formed complexes was examined by applying the continuous variation (Job plot) method [27]. The stoichiometry of the inclusion complexes was assessed by continuous variation method (Job's method) by varying the mole fraction of each component ( $R = [\text{MFA}]/([\text{MFA}] + [\text{HP-}\beta\text{-CD}])$ ) from 0 to 1 and the total molar concentration of the species is kept constant ( $4 \cdot 10^{-5}$  mol/L) [28, 29]. After 48 h samples absorbance was measured at 283 nm, having as blank the solution with the respective CD concentration. The difference in absorbance ( $\Delta A$ ) measured at 283 nm between solutions containing only guest and the MFA/HP- $\beta$ -CD mixtures, multiplied by the molar ratio of MFA was plotted as a function of the  $R$  of guest [30, 31].

### 2.11 Determination of MFA/HP- $\beta$ -CD stability constants

To determinate binding and stability constants for MFA/HP- $\beta$ -CD complexes, a set of MFA absorption spectra in universal buffer solution (pH 7.5) with a fixed concentration of MFA ( $4 \cdot 10^{-5}$  M) and varying concentration of the HP- $\beta$ -CD ( $1.0 \cdot 10^{-3}$ – $2.0 \cdot 10^{-2}$  M) were recorded. The HP- $\beta$ -CD solutions of corresponding concentrations were used in the reference cuvette. Since the observed optical density was always proportional to the concentration of the absorption species, the apparent binding constant ( $K_b$ ) could be determined according to the Benesi-Hildebrand method [32]. The quantitative determination of the  $K_b$  of the inclusion complexes was done at four different temperatures (293 K, 298 K, 310 K).  $K_b$  of the MFA/HP- $\beta$ -CD complex formation can be determined from the plot of  $1/\Delta I$  versus  $1/[\text{HP-}\beta\text{-CD}]$  according to Eq. (3) [33]:

$$\frac{1}{\Delta I} = \frac{1}{a[\text{MF}]} \times \frac{1}{[\text{HP} - \beta - \text{CD}]} + \frac{1}{a[\text{MF}]} \quad (3)$$

$\Delta I$  was calculated according to Eq. (4):

$$\Delta I = I - I_0, \quad (4)$$

where  $I$  and  $I_0$  are the absorbance of the MFA in the solutions with and without HP- $\beta$ -CD, respectively.  $[\text{MFA}]$ ,  $[\text{HP-}\beta\text{-CD}]$  are the initial concentration of MFA, HP- $\beta$ -CD, and  $\Delta a$  is the difference between the molar absorption coefficient of MFA and HP- $\beta$ -CD, respectively. As seen in Eq. (3), the binding constant  $K_b$  can be determined by plotting  $1/\Delta I$  versus  $1/[\text{HP-}\beta\text{-CD}]$  as a line slope.

The stability constant ( $K_S$ ) was determined according to Eq. (5).

$$K_S = \frac{1}{K_b}. \quad (5)$$

## 3. Results and discussion

### 3.1. Characterization of the MFA/HP- $\beta$ -CD complex in liquid state

The MFA/HP- $\beta$ -CD complex was prepared as described above and effects of HP- $\beta$ -CD on MFA solubility and some other parameters were analyzed.

The phase solubility diagram for the created MFA/HP- $\beta$ -CD complexes is shown in Fig. 2 and indicates that the water solubility of the MFA drug increases linearly as a function of the HP- $\beta$ -CD content.

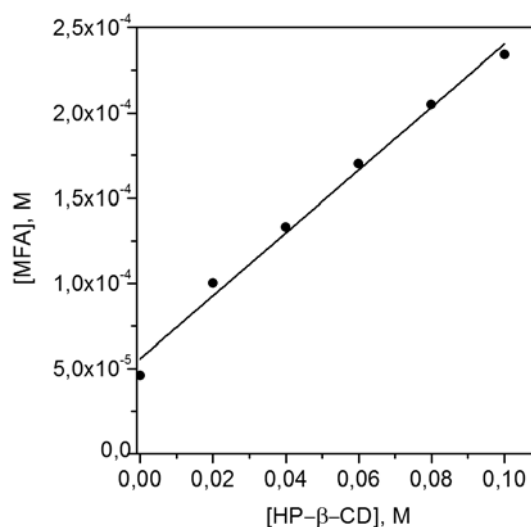


Fig. 2. Phase-solubility diagram for MFA/HP- $\beta$ -CD host-guest system in water at 25°C.

This type of phase solubility diagram of drug and  $\beta$ -CD can be considered as AL type according to Higuchi and Connors [25]. The slope is less than 1 (0.00185), so the solubility enhancement can be attributed to the formation of the first-order MFA/HP- $\beta$ -CD complex with 1:1 stoichiometry [26]. In the presence of 0.1 M HP- $\beta$ -CD, the MFA solubility increases in 4 times. Our data correlate with the data of some authors. Similar phase solubility profiles and solubility enhance ratio have been found by Urszula Domanska et al. [34]. The authors observed an increase in the solubility of MFA to 4.6 times in the presence of HP- $\beta$ -CD at pH 7.0 and a temperature of 298 K. Dounia Sid et al. [35] also reported other similar solubility enhance ratio for MFA and  $\beta$ -cyclodextrin, solubility was increased up to 3.8-fold for MFA in water.

The apparent stability constant ( $K_S$ ) of the MFA/HP- $\beta$ -CD complex was calculated from the linear plot of the phase solubility diagram (Fig. 2) using Eq. (1), and is equal to  $33.0 \text{ M}^{-1}$ . Small  $K_S$  values indicate weak interactions, whereas high  $K_S$  values indicates the limited drug release from the complex. The optimal values of  $K_S$  are considered to be in the range of  $100$ – $1000 \text{ M}^{-1}$  [36]. The complexation efficiency of MFA with HP- $\beta$ -CD was calculated to be 0.002 indicating that approximately one of every 500 cyclodextrin molecules forms a complex with MFA ( $25^\circ\text{C} \pm 0.1^\circ\text{C}$ ). Thus, obtained  $K_S$  value for MFA/HP- $\beta$ -CD complex points to

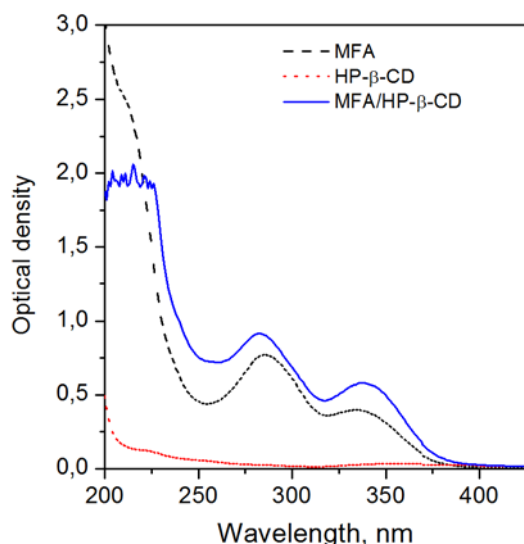


Fig. 3. UV absorption spectra: MFA, HP- $\beta$ -CD and inclusion complex MFA/HP- $\beta$ -CD.

the weak interaction between the components of the host-guest system. At the same time, a fast drug release should be expected.

The MFA/HP- $\beta$ -CD complex formation in aqueous solution was also characterized by UV-vis spectroscopy. The absorption spectra of aqueous solution of MFA, HP- $\beta$ -CD, MFA/HP- $\beta$ -CD are shown in Fig. 3. The obtained curves show that HP- $\beta$ -CD has no absorption in the range of 200–400 nm. In aqueous solution, MFA shows a strong absorption peaks at 286 nm and 335 nm. In the UV spectra of the MFA/HP- $\beta$ -CD the absorption peaks are shifted from 286 to 283 nm and from 335 to 338 nm confirming the formation of MFA/HP- $\beta$ -CD inclusion complexes.

The continuous variation method (Job's plot) was used to confirm the inclusion process and 1:1 stoichiometry as suggested by the solubility experiments. As one can see from Fig. 4, Job's plot for MFA/HP- $\beta$ -CD complex formation is symmetric with the maximum at  $R = 0.5$  that points to the 1:1 stoichiometry of formed complex [27].

The apparent stability constants ( $K_S$ ) of MFA/HP- $\beta$ -CD complexes were calculated by Eq. (5) using the changes in the fluorescence intensity of MFA at 400 nm ( $\Delta I$ ) with different HP- $\beta$ -CD concentrations at different temperatures (293, 298, 310 K). Fluorescence spectra of MFA obtained for different HP- $\beta$ -CD concentrations and at different temperature are presented in Fig. 5. Fluorescence spectra of MFA at pH ~ 7.5 consists of the main band centered at 400 nm and another one centered at 380 nm. The addition of HP- $\beta$ -CD to MFA solution caused remarkable changes in the fluorescence spectra: the increase in intensities of both bands in correlation with increasing HP- $\beta$ -CD concentration. Moreover, the short-wavelength band becomes more intense. The changes in the fluorescence spectra can be ascribed to the formation of the inclusion complexes between MFA and HP- $\beta$ -CD, and transfer of MFA molecule from the polar environment (water) to the non-polar cavity of HP- $\beta$ -CD [37, 38].

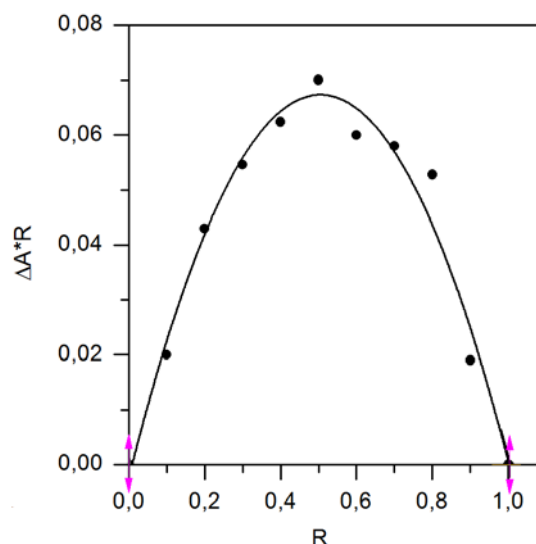


Fig. 4. Continuous variation plot (Job's plot) for the complex formation of MFA with HP- $\beta$ -CD at pH = 7.5.

Since the fluorescence intensity was proportional to MFA concentration,  $K_b$  and  $K_S$  values were calculated using the modified Benesi-Hildebrand equation (Eq. (3) and (4), (5)). Fig. 6 shows the plot of  $1/\Delta I$  versus  $1/[\text{HP-}\beta\text{-CD}]$ . For the considered temperatures good linear correlations were obtained confirming the formation of 1:1 complex.

The  $K_S$  values for different temperatures are given in Table. As one can see the  $K_S$  value for the MFA/HP- $\beta$ -CD complex decreases with increasing temperature, as expected for an exothermic process. This fact can be caused by hydrogen bonds which usually are weakened by heating, suggesting a lower interaction between MFA and HP- $\beta$ -CD at higher temperatures.

The values of entropy ( $\Delta S^0$ ) and enthalpy ( $\Delta H^0$ ) changes of MFA/HP- $\beta$ -CD complex formation were determined from

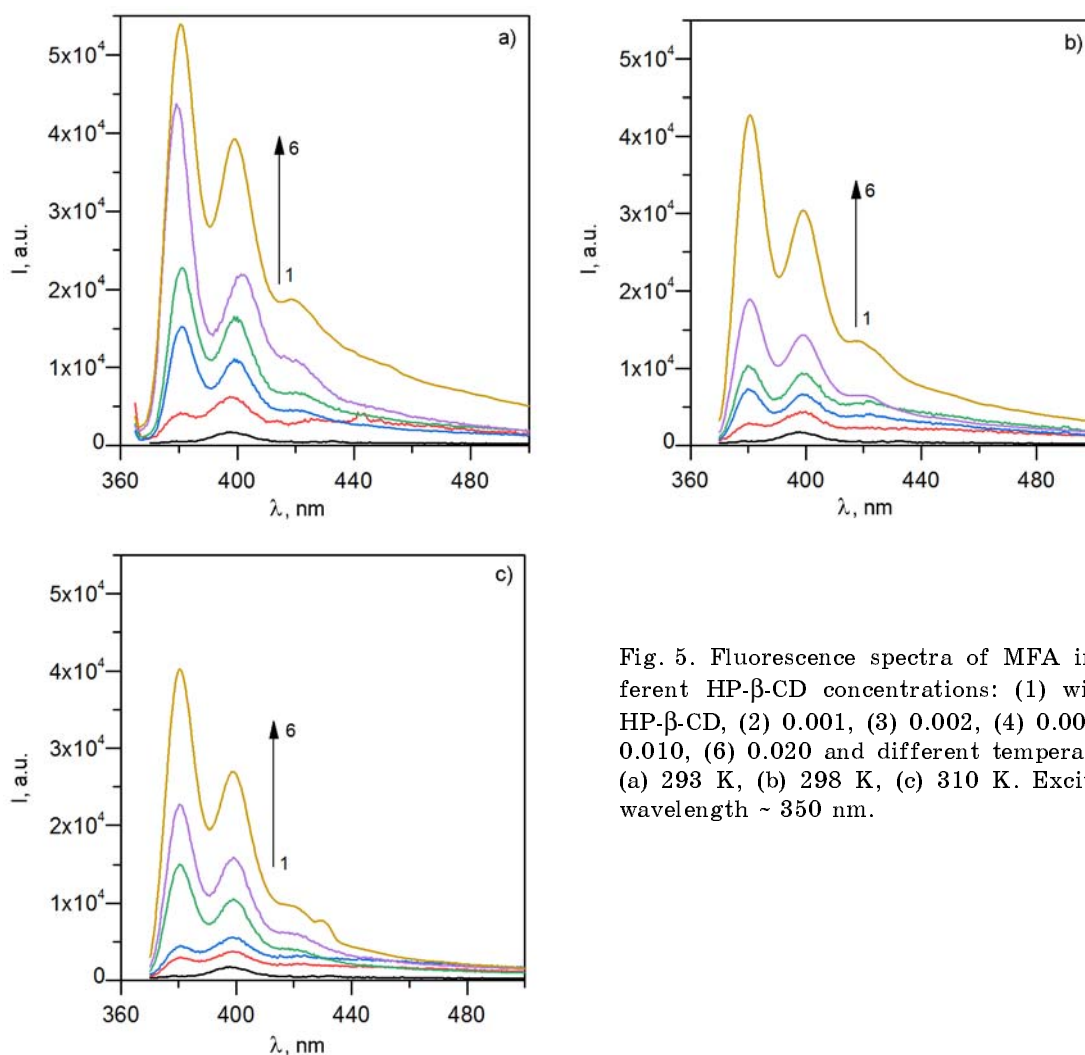


Fig. 5. Fluorescence spectra of MFA in different HP- $\beta$ -CD concentrations: (1) without HP- $\beta$ -CD, (2) 0.001, (3) 0.002, (4) 0.005, (5) 0.010, (6) 0.020 and different temperatures: (a) 293 K, (b) 298 K, (c) 310 K. Excitation wavelength  $\sim 350$  nm.

the temperature dependence of the stability constant i.e.  $\ln K_S$  against  $1/T$  (Fig. 7) using the van't Hoff equation [39]:

$$\ln K_S = -\frac{\Delta H^0}{RT} + \frac{\Delta S^0}{R}, \quad (6)$$

Table. Values of thermodynamic parameters (the stability constant  $K_S$ , the standard molar enthalpy of binding  $\Delta H^0$ , the standard Gibbs free energy change  $\Delta G^0$  and the standard entropy change  $\Delta S^0$ ) of 1:1 complex formation of MFA with HP- $\beta$ -CD in water

$T$ , K	$K_S$ , $M^{-1}$	$\Delta G^0$ , kJ/mol	$\Delta H^0$ , kJ/mol	$\Delta S^0$ , kJ/mol·K
293	184	-12.7		
298	84	-11.0	-68.2	-0.190
310	38	-9.4		

where  $K_S$  is the stability,  $R$  is the gas constant and  $T$  is temperature in Kelvin degrees.

The other thermodynamic parameters such as the free energy ( $\Delta G^0$ ) of complex formation were estimated on the basis of well-known thermodynamic equation:

$$\Delta G = -RT \ln K_S \quad (7)$$

and the obtained thermodynamic parameters are presented in Table.

The  $\Delta G^0$  values provide information whether the reaction conditions are favorable or unfavorable for organic molecules solubilization in the aqueous host solution. The negative  $\Delta G^0$  value obtained for MFA/HP- $\beta$ -CD complex suggests that the binding process is favorable and spontaneous, whereas negative value of  $\Delta H^0$  and  $\Delta S^0$  indicate that the MFA inclusion into HP- $\beta$ -

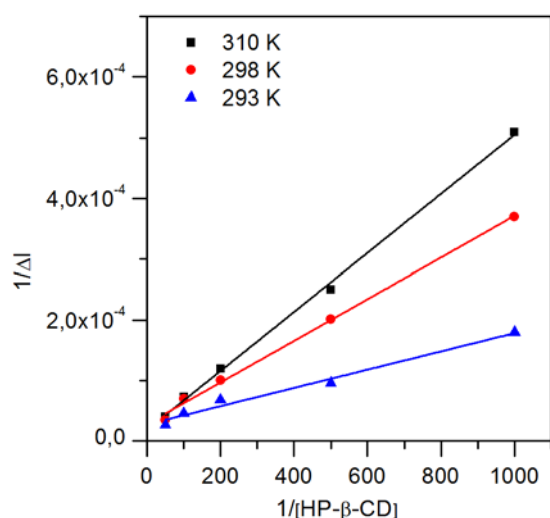


Fig. 6. The plot of  $1/\Delta I$  vs  $1/[\text{HP-}\beta\text{-CD}]$  for MFA/HP- $\beta$ -CD complex formation at different temperatures.

CD cavity is enthalpy-controlled processes in which low energy interactions play an important role.

Different molecular forces are known to be involved into complex formation between cyclodextrins and various molecules. The inclusion complex formation in an aqueous solution results in the rearrangement and removal of the water molecules from the cyclodextrin central cavity accompanied by a change in the electrostatic interactions. The formation of an inclusion complex with cyclodextrin is usually caused by such interactions as hydrogen bonding with -OH groups at the periphery of the CD cavity, van der Waals interactions and hydrophobic effects [40]. CD-inclusion process is usually associated with a negative  $\Delta H^0$ , while  $\Delta S^0$  change could be either positive or negative. The binding event can be decomposed into the solvent- and solute-associated processes. During the binding, some fraction of the surface of both molecules is removed from the contact with solvent and solvent being formerly in contact with molecules returns to the bulk water [41]. The negative values of  $\Delta S^0$  for MFA/HP- $\beta$ -CD complex formation processes are the result of a decrease in translational and rotational degrees of freedom of the complex formation molecules as compared with the free ones, giving more ordered system. Furthermore, the inclusion complexation involves desolvation of both MFA and cyclodextrin, which takes place when MFA penetrate fully inside the CD cavity [42].

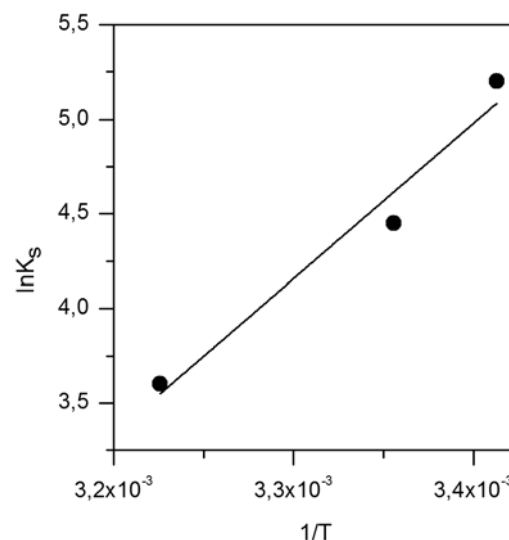


Fig. 7. Van't Hoff graph for MFA/HP- $\beta$ -CD complex formation.

### 3.2. Characterization of the MFA/HP- $\beta$ -CD complex in solid state

To obtain more information about the efficiency of MFA/HP- $\beta$ -CD complex formation, the powders of the complexes were also characterized.

SEM is a qualitative method used to visualize the surface texture of raw materials or the prepared products. The SEM images of the MFA, HP- $\beta$ -CD and inclusion complexes are shown in Fig. 8 (a-c). Pure MFA appeared as irregular-shaped crystals with the flake-like surface (Fig. 8a), whereas HP- $\beta$ -CD are spherical particles with a cavity-like structure (Fig. 8b). In contrast, microscopic observation of the inclusion complex revealed sufficient morphological changes. The inclusion complex (Fig. 8c) reveals bulky prismatic shape with a smooth surface. These morphological changes are useful evidence of interactions between molecules.

DSC is an important criterion for the recognition and characterization of HP- $\beta$ -CD inclusion complexes. When guest molecules are embedded in  $\beta$ -CD cavities, their melting, boiling or sublimating points generally shift or disappear completely [43, 44]. Fig. 9 shows the DSC curves of MFA, HP- $\beta$ -CD, and the MFA/HP- $\beta$ -CD solid complexes obtained by the physical mixing and co-evaporation methods. The DSC curve of pure MFA drug was typical anhydrous crystalline substance exhibiting a flat initial profile followed by a sharp melting endotherm at about 231°C. The DSC profile of



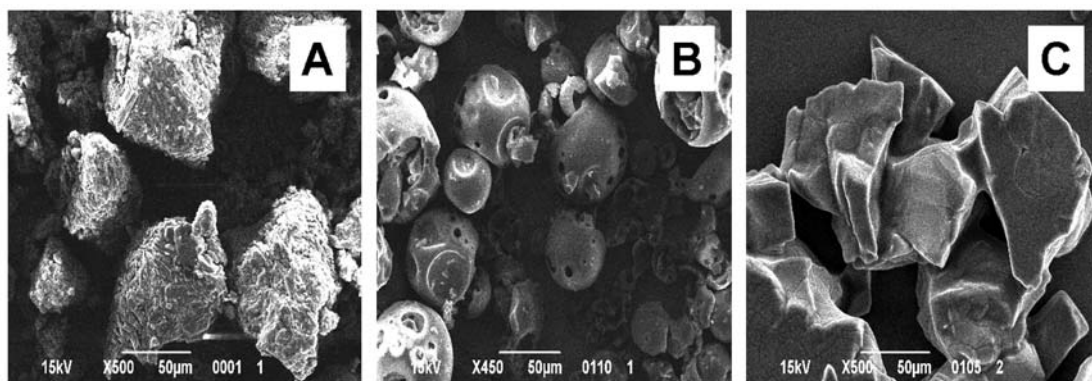


Fig. 8. SEM images: (a) pure MFA, (b) HP- $\beta$ -CD, (c) MFA/HP- $\beta$ -CD complex.

HP- $\beta$ -CD showed a large endothermic peak associated with water loss between 80 and 120°C (Fig. 9b). These results are in accordance with [45]. For the solid complex obtained by the physical mixturing the apparent endothermic MFA transition (the shift of the endothermic peak to 220°C) was observed (Fig. 9d) indicating the weak interactions between MFA and HP- $\beta$ -CD. However, this melting endotherm completely disappeared in the thermogram of inclusion complex obtained by co-evaporation (Fig. 9c) and this result indicates a successful complexation of MFA and HP- $\beta$ -CD.

The TGA curves of HP- $\beta$ -CD, MFA, MFA/HP- $\beta$ -CD are shown in Fig. 10. At 105°C HP- $\beta$ -CD has weight loss of 7.0 % attributed to water evaporation. Furthermore, for MFA/HP- $\beta$ -CD water loss (7.5 %) was slower than for HP- $\beta$ -CD suggesting that the water — cyclodextrin interactions in inclusion complex are stronger. The inhomogeneity of the samples in terms of the content of volatile impurities was 0.4 %.

The interaction between the drug molecules and hydrophobic CD nanocavities in solid state was investigated by FTIR spectroscopy. Inclusion complex formation is generally identified by intensity changes, disappearance, and widening, as well as shifting of peaks. The FTIR spectra of MFA, HP- $\beta$ -CD, physical mixture and MFA/HP- $\beta$ -CD are shown in Fig. 11. In the spectrum of HP- $\beta$ -CD, the major absorption peaks were observed at 1020, 1070 and 1150  $\text{cm}^{-1}$  corresponding to the coupled C—C/O stretching vibrations and the anti-symmetric stretching vibration of the C—O—C glycosidic bridge of HP- $\beta$ -CD molecules [46]. The most characteristic peaks of HP- $\beta$ -CD relate to OH stretching (3400  $\text{cm}^{-1}$ ), CH

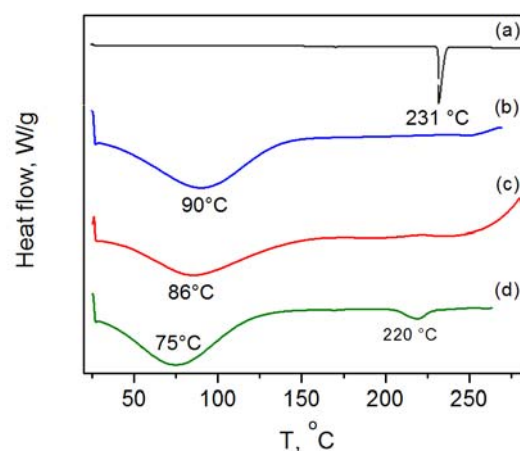


Fig. 9. DSC curves of MFA a) HP- $\beta$ -CD, b) MFA/HP- $\beta$ -CD complex c), physical mixture MFA with HP- $\beta$ -CD d).

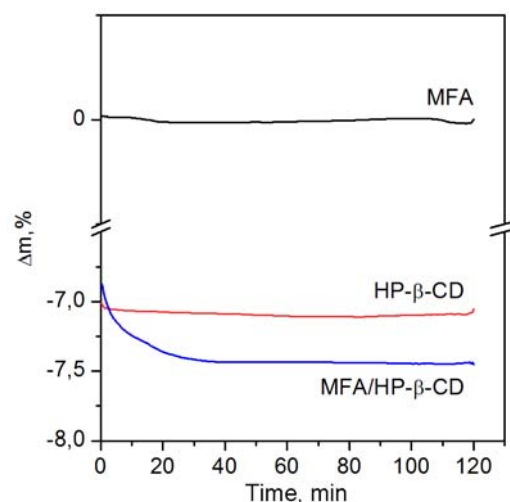


Fig. 10. TGA of mass losses for MFA, HP- $\beta$ -CD, MFA/HP- $\beta$ -CD complex at 105°C.

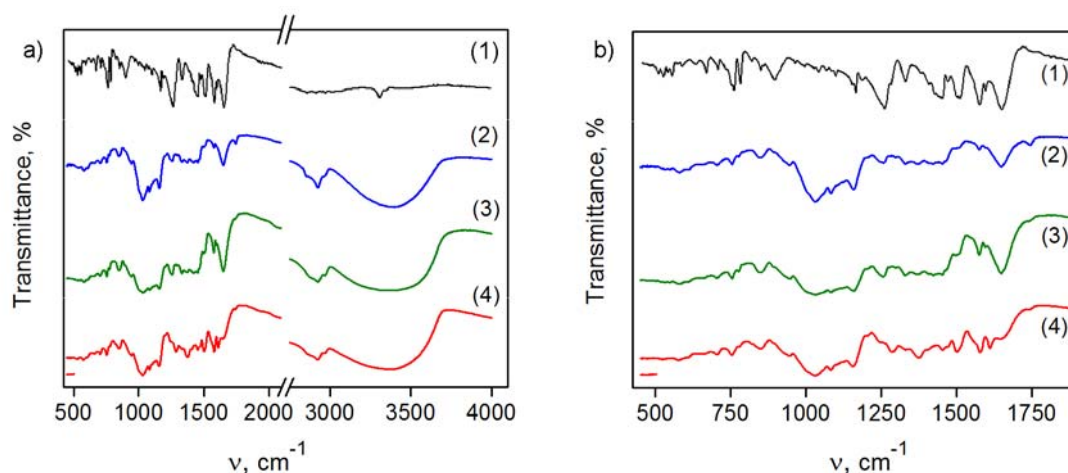


Fig. 11. FTIR spectra of (a) MFA 1), HP- $\beta$ -CD, 2) physical mixture MFA with HP- $\beta$ -CD, 3) MFA/HP- $\beta$ -CD complex 4) and (b) FTIR spectra in the low frequency region.

stretching ( $2930\text{ cm}^{-1}$ ) and C=O stretching ( $1640\text{ cm}^{-1}$ ) [47]. The broad peak at  $3400\text{ cm}^{-1}$  could be attributed to the influence of hydrogen bonding.

The FTIR spectrum of pure MFA is presented in Fig. 11a. The band at  $3312\text{ cm}^{-1}$  arises from the amino group internally hydrogen bonding with the carbonyl group [48]. Besides, other bands were observed at  $1649\text{ cm}^{-1}$  for C=O stretching vibration and at  $1257\text{ cm}^{-1}$  for C–N stretching vibration. The strong C=C stretching vibrations of the aromatic ring appeared at  $1575\text{ cm}^{-1}$ ,  $1510\text{ cm}^{-1}$ ,  $1472\text{ cm}^{-1}$  and  $1450\text{ cm}^{-1}$  along with four weak bands for the overtones and combinations at  $2000\text{--}1700\text{ cm}^{-1}$ . The bands at  $1193\text{ cm}^{-1}$ ,  $1162\text{ cm}^{-1}$ ,  $1083\text{ cm}^{-1}$ ,  $1064\text{ cm}^{-1}$ ,  $1036\text{ cm}^{-1}$ ,  $778\text{ cm}^{-1}$  and  $754\text{ cm}^{-1}$  are related to CH in-plane bending and CH out-of-plane bending vibrations of aromatic ring [48].

The spectrum of the physical mixture of MFA and HP- $\beta$ -CD in the range from  $1650$  to  $1257\text{ cm}^{-1}$  is similar to the combination of the MFA and HP- $\beta$ -CD spectra (Fig. 11b). Remarkably, the NH stretching vibration, the overtones and combination bands for the aromatic ring and the strong band for C–N stretching vibration ( $1257\text{ cm}^{-1}$ ) completely disappeared in inclusion complexes. Further the strong band for C=O stretching ( $1650\text{ cm}^{-1}$ ) was shifted to  $1612\text{ cm}^{-1}$  in the MFA/HP- $\beta$ -CD complexes suggesting that the methyl substituted aromatic ring along with the amine (NH) group may be included into the CD nanocavity.

#### 4. Conclusions

Taking all experimental results together, we can conclude that in water solutions MFA effectively forms an inclusion complex with HP- $\beta$ -CD that increase drastically the solubility of MFA. UV-vis spectral data and phase-solubility studies indicated that MFA forms a complex with the HP- $\beta$ -CD at a 1:1 molar ratio and the apparent stability constant is adequate for the formation of an inclusion complex that may contribute to improving the bioavailability of a poorly water-soluble drug like MFA. The thermodynamic data estimated using the van't Hoff equation confirm that the MFA/HP- $\beta$ -CD complex formation is thermodynamically favorable and exhibits a negative change in Gibbs free energy. In addition, MFA/HP- $\beta$ -CD complex formation is endothermic and entropy driven process. The solid complex was prepared by the co-evaporation method. Characterizations of the prepared host-guest type solid complexes using FTIR, DSC, TGA and SEM methods indicate that MFA is found inside the cavity of the HP- $\beta$ -CD.

**Acknowledgements.** This work was supported by National Academy of Sciences of Ukraine within the Target Program of Scientific Research of NAS of Ukraine "Materials for Medicine and Medical Equipment and Technologies for their Production and Use" (Project No.0117U006245).

#### References

1. G.C.Seuanez, M.B.Moreira, T.Petta et al., *J. Inorg. Biochem.*, **153**, 178 (2015).
2. G.Ribeiro, M.Benadiba, A.Colquhoun, D.D.Silva, *Polyhedron*, **27**, 1131 (2008).

3. S.Bindu, S.Mazumder, U.Bandyopadhyay, *Biochem. Pharmacol.*, **180**, 11447 (2020).
4. V.R.Cunha, C.M.Izumi, P.A.Petersen et al., *J. Phys. Chem. B*, **118**, 4333 (2014).
5. D.K.Demertzi, D.H.Litina, M.Staninska et al., *J. Enzyme Inhib. Med. Chem.*, **24**, 742 (2009).
6. A.D.S.Hernandez, H.R.G.Salazar, D.A.M.Galindo et al., *Int. Urol. Nephrol.*, **44**, 471 (2012).
7. D.H.Woo, I.S.Han, G.Jung, *Life Sci.*, **24**, 2439 (2004).
8. M.Asanuma, S.Nishibayashi-Asanuma, I.Miyazaki et al., *J. Neurochem.*, **76**, 1895 (2001).
9. O.Bekers, E.V. Uijtendaal, D.A.Beijnen et al., *Drug Dev. Ind. Pharm.*, **17**, 1503 (2008).
10. K.Lobmann, H.Grohgan, R.Laitinen et al., *Eur. J. Pharm. Biopharm.*, **85**, 873 (2013).
11. G.L.Amidon, H.Lennernas, V.P.Shah, J.R.Crisson, *Pharm. Res.*, **12**, 413 (1995).
12. M.N.Anjana, J.Joseph, S.C.Nair, *Int. J. Pharm. Sci. Rev. Res.*, **20**, 127 (2013).
13. A.R.Hedges, *Chem. Rev.*, **98**, 2035 (1998).
14. K.A.Connors, *Chem. Rev.*, **9**, 1325 (1997).
15. E.M.M.Del Valle, *Process. Biochem.*, **39**, 1088 (2004).
16. J.Szejtli, *Chem. Rev.*, **98**, 1743 (1998).
17. N.Qiu, X.B.Li, J.D.Liu, *J. Incl. Phenom. Macrocycl. Chem.*, **89**, 229 (2017).
18. M.E.Brewster, T.Loftsson, *Adv. Drug Deliv. Rev.*, **59**, 645 (2007).
19. S.Gould, R.C.Scott, *Food Chem. Toxicol.*, **43**, 1451 (2005).
20. J.Szejtli, *Pure Appl. Chem.*, **76**, 1825 (2004).
21. L.Liu, Q.Guo, *J. Incl. Phenom. Macrocycl. Chem.*, **42**, 1 (2002).
22. T.Yousef, N.Hassan, *J. Incl. Phenom. Macrocycl. Chem.*, **87**, 105 (2017).
23. C.T.Chang, L.C.Chen, C.C.Chang et al., *J. Clin. Pharm. Ther.*, **33**, 495 (2008).
24. V.R.Sinha, Amita, R.Chadha et al., *Cent. Eur. J. Chem.*, **8**, 953 (2010).
25. T.Higuchi, K.A.Connors, *Phase Solubility Techniques*, Interscience, New York (1965).
26. T.Loftsson, D.Hreinsdottir, M.Masson, *J. Incl. Phenom. Macrocycl. Chem.*, **57**, 545 (2007).
27. P.Job, *Ann. Chim.*, **9**, 113 (1928).
28. J.S.Renny, L.L.Tomasevich, E.H.Tallmadge, D.B.Collum, *Angew. Chem. Int. Ed.*, **52**, 11998 (2013).
29. H.Bouzit, M.Stiti, M.Abdou, *J. Incl. Phenom. Macrocycl. Chem.*, **86**, 121 (2016).
30. W.Misiuk, M.Zalewska, *J. Mol. Liq.*, **159**, 220 (2011).
31. J.V.Caso, L.Russo, M.Palmieri et al., *Amino Acids*, **47**, 2215 (2015).
32. H.A.Benesi, J.H.Hildebrand, *J. Am. Chem. Soc.*, **89**, 2703 (1949).
33. S.Hamai, *Bull. Chem. Soc. Jpn.*, **55**, 2721 (1982).
34. U.Domanska, A.Pelczarska, A.Pobudkowska, *Int. J. Mol. Sci.*, **12**, 2383 (2011).
35. D.Sid, M.Baitiche, Z.Elbahri et al., *J. Enzyme Inhib. Med. Chem.*, **36**, 605 (2021).
36. R.Arun, K.C.K.Ashok, V.V.N.S.S.Sravanthi, *Scientia Pharmaceutica*, **76**, 567 (2008).
37. R.Periasamy, S.Kothainayaki, K.Sivakumar, *J. Mol. Struct.*, **1080**, 69 (2015).
38. R.Rajamohan, S.Kothai Nayaki, M.Swaminathan, *J. Mol. Liq.*, **220**, 918 (2016).
39. P.Padhan, A.Sethy, P.K.Behera, *J. Photochem. Photobiol. A*, **337**, 165 (2017).
40. A.M.Stalcup, S.S.Chang, D.W.Armstrong, J.Pitha, *J. Chromatogr.*, **513**, 181 (1990).
41. M.C.Chervenak, E.J.Toone, *J. Am. Chem. Soc.*, **116**, 10533 (1994).
42. C.Alvariza, R.Usero, F.Mendicuti, *Spectrochim. Acta A*, **67**, 420 (2007).
43. R.Singh, N.Bharti, J.Madan, S.N.Hiremath, *J. Pharm. Sci. Technol.*, **2**, 171 (2010).
44. L.Liu, S.Zhu, *J. Pharm. Biomed. Anal.*, **40**, 122 (2006).
45. S.Siva, S.Kothai Nayaki, N.Rajendirana, *Spectrochim. Acta Part A*, **174**, 349 (2017).
46. A.Celebioglu, T.Uyar, *J. Agric. Food Chem.*, **65**, 5404 (2017).
47. N.Qiu, X.Zhao, Q.Liu et al., *J. Mol. Liq.*, **289**, 111151 (2019).
48. S.Romero, B.Escalera, P.Bustamante, *Int. J. Pharm.*, **178**, 193 (1999).